ISBN: 978-3-95450-179-3 doi:10.18429/JACoW-FEL2017-TUP062

ELECTROMAGNETIC AND MECHANICAL ANALYSIS OF A 14 MM 10-PERIOD NBTI SUPERCONDUCTING UNDULATOR*

F. Trillaud†, Instituto de Ingeniería, UNAM, CDMX, 04510, Mexico
G.A. Barraza-Montiel, Facultad de Ingeniería, UNAM, CDMX, 04510, Mexico
M. Gehlot, and G. Mishra, IDDL, Devi Ahilya University, Indore, MP 452001, India

Abstract

A 14 mm - 10 period NbTi superconducting undulator for the next generation of Free Electron Laser has been studied. The optimum electromagnetic pre-design was carried out using RADIA, an extension module of the commercial software Mathematica. For this pre-design, a variable gap was considered. Additionally, a thermo-mechanical study of one eighth of the superconducting undulator was conducted. This study utilized a thermal and mechanical contact model between the pancake coils and the carbon steel core. This coupled model allowed estimating the minimum pre-loading of the coil. This pre-loading ensures that the coil would remain stuck to its pole during cooling. Numerical results are presented for both studies.

INTRODUCTION

The new generation of light sources are expected to achieve greater luminosity benefiting from the advances in superconducting wires and tapes [1]. In the past 15 years, an increasing body of research has been dedicated to the development of superconducting insertion devices making use of state of the art commercial Low Temperature Superconductors operated in liquid helium [2]. Over the years, a few prototypes have been built and installed showing the applicability of the technology [3]. As the superconductivity gets more and more reachable to countries such as India which operates light sources, there is an increasing interest in exploring new technologies to upgrade their existing facilities [4]. It should be noted that the Mexican scientific community, users of light sources, have recently expressed their interest in the construction of a first light source in Mexico [5]. Addressing both interests in light sources and new technological developments for greater brightness, a small program to develop a first Indian 14 mm-10 period superconducting undulator operated in boiling liquid helium at 4.2 K has been launched in 2015 [6, 7], a technology that will certainly benefit the Mexican light source as well.

SCU are superconducting electromagnets wound on two ferromagnetic cores separated by a gap. The electromagnets are made of series-connected, impregnated coils with alternative winding to provide an oscillating magnetic field on axis [8]. The magnitude of the field is adjusted by the current intensity fed to the coils. Additionally, as the superconductor can carry large amount of currents without losses, it is possible to achieve greater field allowing the construction of shorter period undulators at a greater brightness than any of the conventional technologies [9]. They are clear advantages over more conventional technologies such as permanent magnets (PPM) and hybrid undulators (HU).

The following work reports pre-studies carried out on a NbTi undulator to be operated at 4.2 K and its structure. The choice of the conductor was made on the basis of its well-understanding and its malleability compared to other technologies such as Nb_3Sn or the High Temperature Superconductors (HTS) [10, 11]. The electromagnetic pre-design, the conceptual design of the mechanical structure and cryogenic system needed to test the SCU and a mechanical pre-analysis to operate safely the device are presented. The current margin of the superconducting electromagnet and the pre-compression to ensure that the coils would not delaminate from their support were estimated. It is a first step allowing understanding the technology to be completed by more in depth studies.

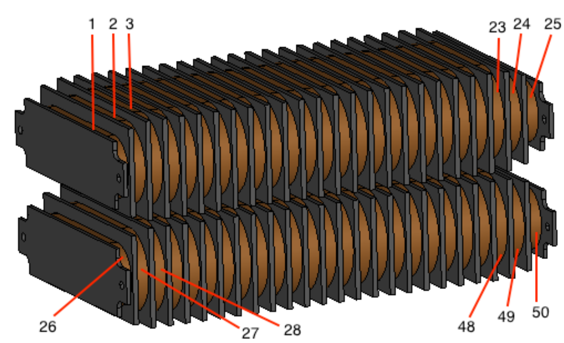

Figure 1: SCU structure with coil packs.

ELECTROMAGNETIC PRE-DESIGN

The NbTi superconducting undulator (SCU) is composed of two separated carbon steel cores, referred to as poles as it is shown in Fig. 1. Each pole holds 25 epoxy-impregnated racetrack coils connected in series with alternative winding. The coils are numbered from 1 to 50 over both poles (1-25 and 26-50). The first and last two coils of each pole are graded to smoother the magnetic flux density and lower the kick. The first and last coils (1 and 25, 26 and 50) are 1/4th of the height and width of the regular coil whereas the second and the penultimate coils (2 and 24, 27 and 49) are 3/4th. The regular coils, 3-23 and 28-48, have same dimensions along the pole length to generate a regular oscillating magnetic field. Figure 2 provides the dimensions of a regular coil and

* Work supported by the Dirección General Asuntos del Personal Académico (DGAPA) of the Universidad Nacional Autónoma de México (UNAM) under grant PAPIIT TA100617 and from SERB, India.
† ftrillaudp@iingen.unam.mx

ISBN: 978-3-95450-179-3 doi:10.18429/JACoW-FEL2017-TUP062

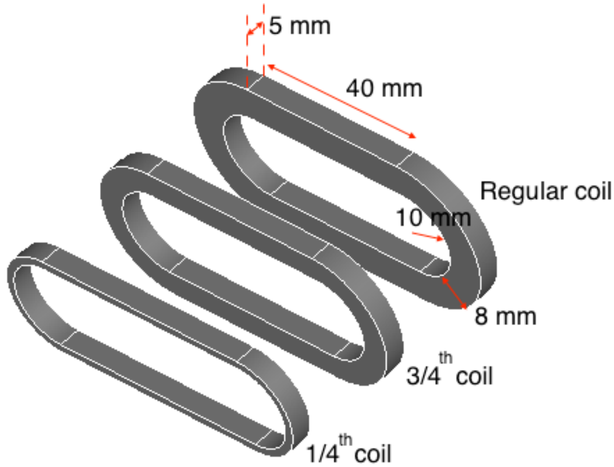

Figure 2: Dimensions of the regular coil. The 3/4th and 1/4th have same cross-section but their length and width are scaled down.

shows the scale of the graded coils compared to this same regular coil. Each coil is separated by a 2 mm thick carbon steel wall whose widths and heights are the same as the coil ones.

The module RADIA of the commercial software Mathematica [12] was used to provide a first estimation of the current margin of the superconducting electromagnet. The geometry of the SCU was meshed and the magnetic flux density was computed on axis and off axis at the surface of the coil. The results provided the choice of the commercial superconductor and the distance between the ferromagnetic cores to ensure a safe operation of the SCU at 4.2 K. Amongst some of th most relevant results are given in Figs. 3 and 4. The former shows the engineering current density flowing through the SCU as a function of the magnetic flux density on the coil and the latter 4 shows the evolution of the magnitude of the magnetic flux density on axis. Using both figures, an insulated rectangular 1 mm x 0.5 mm conductor with a copper-to-superconductor ratio equal to 1.5 was chosen to reach a target of 1 T on axis with a current margin on the superconductor larger than or equal to 10% at a gap of 5 mm for an engineering current density in the superconductor of 800 A/mm^2 [7].

CONCEPTUAL DESIGN OF THE MECHANICAL STRUCTURE AND CRYOGENIC SYSTEM

Figure 5 shows the conceptual design of the cryogenic experimental setup to test the proposed SCU in liquid helium (LHe) at 4.2 K. The experimental setup is composed of a LHe cryostat surrounded by a liquid nitrogen jacket (LN_2). A top flange, which seals the cryostat, houses two vapor-cooled current leads, sealed connectors for data transfer, LHe level sensor, a LHe inlet and a relief valve for safety purposes. Four non-magnetic rods, screwed to the top flange, hold the SCU in a vertical position. Cu plates and a styrofoam ring are used to scatter the convection heat transfer and are

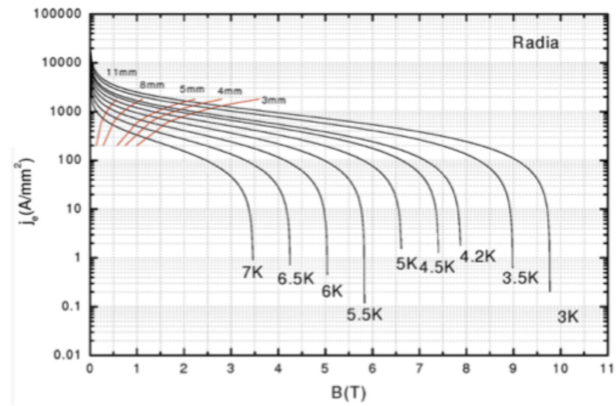

Figure 3: Current margin on the superconductor at different gaps [7].

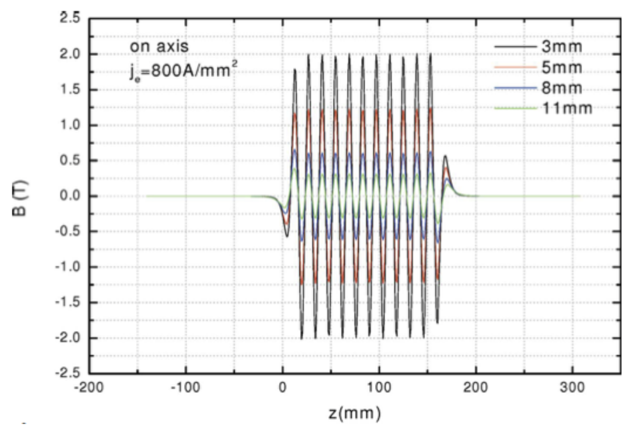

Figure 4: Pattern of the magnetic flux density generated by the SCU. By grading the coils, the kick is smoothed allowing a stable entrance and exit of the electron beam [7].

held by the same rods supporting the undulator. A G10 plate allows centering the experiment and guiding the rods. Spring-like supports at the extremities of the SCU poles will be considered to ensure that the gap remains equal to 5 mm during cooling and energizing. Various thermal sensors, labeled T_1 through T_4 will be installed at key locations to monitor the cooling of the system. A 5-V, 600-A power supply feeds the vapor-cooled current leads connected to the undulator winding, producing an adequate magnetic field in the gap between the undulator poles.

A magnetic rig, consisting of an infinite screw linear positioner and an array of Hall probes, will allow to measure the magnetic field between the undulator poles. This feature will slide along the undulator gap to perform the field mapping at different locations. A crane will help holding the top flange and a special stand is used to help positioning the undulator so that the operator can easily connect the undulator to the rods and the current leads. Once the undulator is attached to the experimental holder (top flange and its components) and connected to the current leads, the holder is dipped into the cryostat using the crane. The cryostat is then slowly filled up with LHe meanwhile the temperature across the system is monitored.

ISBN: 978-3-95450-179-3 doi:10.18429/JACoW-FEL2017-TUP062

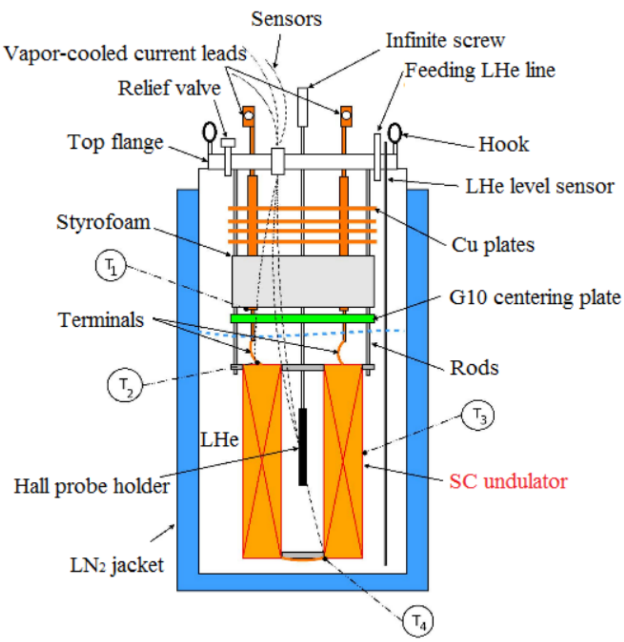

Figure 5: Conceptual design of the experiment setup to test the proposed SCU.

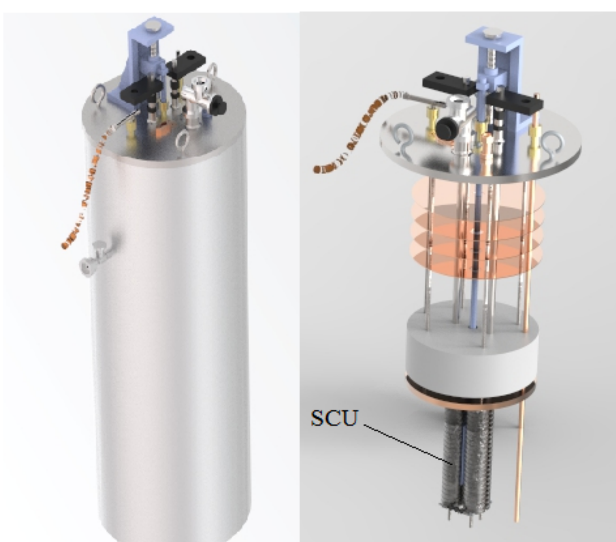

Figure 6: 3D CAD of the experimental setup showing detailed engineered parts and the SCU.

Figure 6 shows the corresponding 3D solid model of the SCU experiment. This setup is expected to be built upon grant approval.

THERMO-MECHANICAL ANALYSIS

A coupled thermo-mechanical 3D Finite Element Analysis (FEA) of the SCU was conducted using the electromagnetic pre-design as geometrical input. The model assumed non-ideal thermal and mechanical contacts between the coils and their pole. For each time step, the temperature distribution was first computed assuming a cooling speed of 30 min. Then, the mechanical strains and stresses were calculated from the thermal induced deformation. A pre-compression was added to the mechanical model to simulate the winding tension and an eventual additional wrapping on top of the coils. Such a wrapping can be made of aluminum having a larger thermal contraction than the coil winding providing an adjustable pre-loading. In the model, the magnitude of the pre-compression is tuned so that the coils remain in contact to the surface of the core.

Thermal Model

The heat balance equation to solve the temperature field of the SCU is given by

$$\nabla . [k\nabla (T)] = \rho c_p \frac{\partial T}{\partial t} \quad (1)$$

where T is the temperature, ρ the mass density, k the thermal conductivity and c_p the specific heat capacity, both depending on temperature. To model the thermal properties of the winding, it is necessary to take into account the properties of the different materials: superconductor, Cu matrix, insulation and epoxy. To that end, a mixture rule was applied to obtain an isotropic, homogeneous equivalent material property of the coils. In addition, the thermal contact between coils and poles was added to the model through an equivalent thermal heat exchange coefficient h so that

$$\Delta\Phi_{\mathrm{j,i}} = h\left(T_{\mathrm{j}} - T_{\mathrm{i}}\right) \quad (2)$$

is the exchanged heat flux in W/m^2 between the surfaces i and j in contact. The value of the equivalent thermal heat exchange coefficient was chosen equal to 2580 W/m^2-K [13].

To simulate the cooling down of the device from room temperature to 4.2 K, a time varying boundary condition was applied to the external surfaces of the SCU model. The expression of the boundary temperature T_{b} is given by

$$T_{\mathrm{b}}(t) = (T_{\mathrm{lh}} - T_0)e^{-\beta t} + T_0 \quad (3)$$

where T_0 is equal to 300 K and T_{lh} represents the liquid helium temperature equal to 4.2 K. β is a parameter associated with the cooling speed in s^{-1}. This parameter was chosen as 0.0045 s^{-1} to provide a slow cooling of 30 min, an achievable cooling speed for the dimensions of the cryogenic system.

Mechanical Model and Thermo-Mechanical Coupling

One of the requirements to ensure a reliable SCU's operation and performance is to avoid a large coil deformation during the different phases of the device operation. These phases include cooling, energizing and warming. In the present work, the focus is on the cooling step where the difference in thermal expansion coefficient between the coil and its support may lead to the loss of contact between the two. This loss of contact may lead to early quenches. It is

ISBN: 978-3-95450-179-3 doi:10.18429/JACoW-FEL2017-TUP062

worth mentioning that during the current loading of the magnet, deformations arising from the Lorentz forces are also expected to occur. This effect will be studied later on. To minimize the risk of coil delamination, a classic strategy is to apply a pre-loading if the winding tension is not enough.

Addressing only the issues related to the cooling phase, the mechanical equation that defines the displacement field $\boldsymbol{u} = [u, v, w]$ due to the thermal load, is given by

$$G\nabla^2\boldsymbol{u} + \frac{G}{1-2\nu}\nabla(\nabla.\boldsymbol{u}) - \frac{E}{1-2\nu}\alpha\nabla(T) = \rho\ddot{\boldsymbol{u}} \quad (4)$$

where E is the Young's Modulus (210 GPa for the carbon steel and 120 GPa for the winding pack), ν is the Poisson's ratio (0.3), $G = E/2(1+\nu)$ is the shear modulus and α is the thermal expansion coefficient (17×10^{-6} K^{-1} for the carbon steel and 9.8×10^{-6} K^{-1} for the winding pack). The contact is modeled through an elastic relation between the displacement of the nodes composing the surface of the material facing each other. No interpenetration is allowed.

The coupling is carried out by adding the thermal strain to the equation of the displacement field (4). The thermal strain depends directly on the coefficient of thermal expansion α and the temperature gradient. This coefficient is similarly obtained by a mixture rule.

The clamping of the SCU to the support rod is modeled through a spring-like boundary condition (spring foundation).

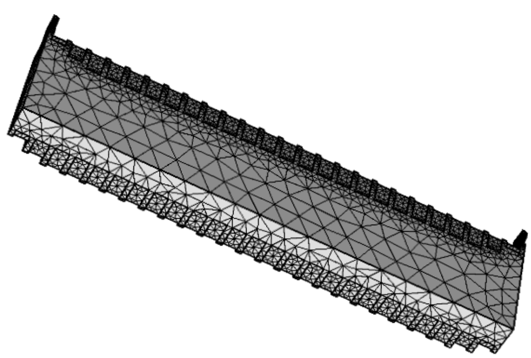

Figure 7: Meshing of 1/8$^{\text{th}}$ of the SCU. A denser mesh is used around the coil to provide a better resolution of the temperature and displacement fields. The same mesh was used for the thermal and mechanical problems.

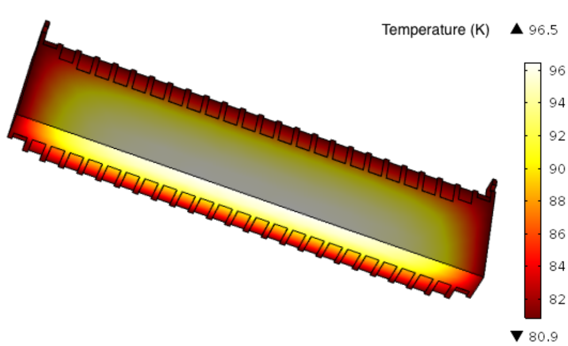

Figure 8: Temperature distribution at 300 s at the beginning of the cooling phase.

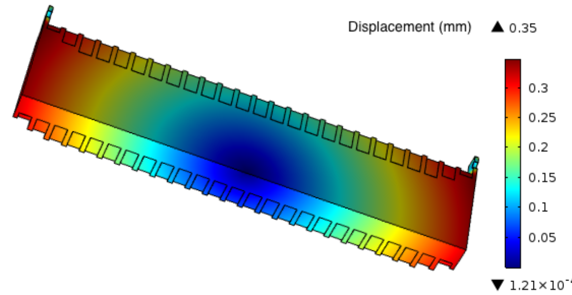

Figure 9: Displacement field at 300 s corresponding to the temperature distribution shown in Fig. 8.

FEA Model and Solver

To solve the 3D coupled temperature and displacement fields, the authors used the commercial FEA software COMSOL Multiphysics® version 5.2. Benefiting from the symmetry of the problem, only one eighth of the SCU was modeled, representing a quarter of a pole. Figure 7 shows the mesh used for the coupled analysis. A small gap exist between the coil and the pole meshes to model both the thermal and mechanical contacts.

The heat balance and field displacement equations are solved sequentially. First, the temperature distribution is obtained, then the thermal strain is computed and added to the mechanical model. The same mesh was used for both the thermal and mechanical models. At each time step, both the temperature and the displacement fields are obtained until steady state is reached.

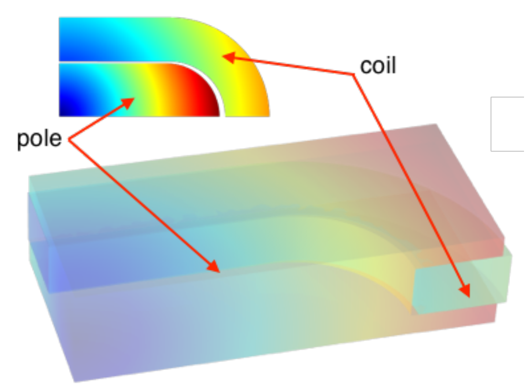

Figure 10: Detail of the coil separation from the ferromagnetic core. The displacement is amplified by a factor of 15.

THERMO-MECHANICAL RESULTS AND DISCUSSION

At first, the whole SCU is at 300 K. For this analysis, it is assumed that the SCU is homogeneously cooled by LHe. As the boundary temperature follows (3), a thermal gradient develops inside the SCU. This thermal gradient vanishes rapidly after the boundary reached 4.2 K. Figures 8 and 9 show the temperature distribution and the displacement field after 300 s at the beginning of the cooling phase, respectively. Because of the discrepancies in the material

ISBN: 978-3-95450-179-3 doi:10.18429/JACoW-FEL2017-TUP062

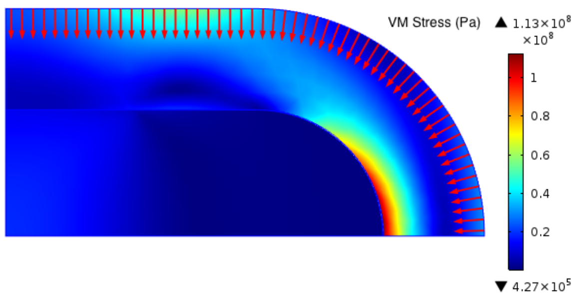

Figure 11: A pre-compression of 25 MPa allows the contact between the inner surface of the coil and its pole. The maximum stress generated at the coil is equal to 113 MPa.

thermal shrinkage, a thermal strain develops that can be ultimately compensated by a pre-loading (or the winding tension). Without pre-loading, if the coil is poorly bonded to its carbon steel support, it is likely to delaminate as shown in Fig. 10. As a result, an overall maximum separation of 0.05 mm occurs at the circular portion of the racetrack coil meanwhile, over the straight section, the separation amounts to a maximum of 0.024 mm. By applying a pre-loading of about 25 MPa as shown in Fig. 11, this separation disappears and the maximum Von Mises stress developed in the coil still reaches an admissible value of 113 MPa [14]. Since the deformations of the coil and the pole remain small, the elastic model provides a good first approximation. However, it should be noted that this model, elastic in its most basic assumption, does not include phenomena such as cracks and fractures. Therefore, the resulting deformation once the temperature of the SCU reached 4.2 K is independent of the cooling velocity. It is a limitation of the model which can difficulty be overcome without experimental data.

CONCLUSION

A preliminary mechanical and magnetic study has been conducted to build a NbTi superconducting undulator prototype to be tested at 4.2 K in liquid helium. This first Indian superconducting prototype is expected to be tested at the Insertion Device Development and Measurement Lab of the Devi Ahilya University. The electromagnetic pre-design targets a 1 T magnetic flux density on axis for a gap of 5 mm. On the basis of field requirement, a rectangular commercial NbTi wire has been chosen which provides a safe temperature and current margin to reach the nominal magnetic field on axis. To avoid the possibility of delamination of the coils during cooling, the magnitude of the pre-compressing force (pre-loading) was estimated. Further works are still necessary to take into the mechanical behavior of the SCU poles during energization. In addition to the thermal forces, the Lorentz force will be added to the mechanical model to get the proper pre-loading.

REFERENCES

[1] N. Mezentsev, "Survey of superconducting insertion devices for light sources," in *Proceedings of PAC'05), Knoxville, Tennessee*, pp. 256–260, 2006.

[2] C.S. Hwang, J.C. Jan, C.S. Chang, S.D. Chen, C.H. Chang, and T.M. Uen, "Development trends for insertion devices of future synchrotron light sources," *Physical Review Special Topics - Accelerators and Beams*, vol. 14, no. 044801, 2011.

[3] E. Moog and Y. Ivanyushenkov, "Developments in superconducting insertion devices," in *Proceedings of PAC'11), New York, NY, USA*, pp. 2077–2081, 2012.

[4] H. Winick, "Synchrotron light sources in developing countries," in *APS March Meeting 2017, New Orleans, Louisiana, USA*, vol. 62, 2017.

[5] A. Antillón, J. Jiménez and M. Moreno, "Momentum gathers towards a Mexican light source," https://www.aps.org/units/fip/newsletters/201509/mexico.cfm. Forum on International Physics, 2015.

[6] M. Gehlot, G. Mishra, F. Trillaud, G. Sharma, "Magnetic design of a 14 mm period prototype superconducting undulator," *Nuclear Instruments and Methods in Physics Research A*, vol. 846, pp. 13–17, 2017.

[7] G. Mishra, M. Gehlot, G. Sharma, and F. Trillaud, "Magnetic design and modelling of a 14 mm-period prototype superconducting undulator," *Journal of Synchrotron Radiation*, vol. 24, pp. 1–7, 2017.

[8] S. Prestemon, D. Dietderich, S. Marks, and R. Schlueter, "NbTi and Nb3Sn superconducting undulator designs," in *AIP Conference Proceedings*, vol. 705, pp. 294–300, 2004.

[9] J. Bahrdt and Y. Ivanyushenkov, "Short period undulators for storage rings and free electron lasers," in *Journal of Physics: Conference Series*, vol. 425, p. 032001, 2013.

[10] P. Emma *et al.*, "A plan for the development of superconducting undulator prototypes for LCLS-II and future FELs," in *Proceedings of FEL'14, Basel, Switzerland*, 2014.

[11] I. Kesgin, C. Doose, M. Kasa, Y. Ivanyushenkov, and U. Welp, "Design of a REBCO thin film superconducting undulator," in *IOP Conference Series: Materials Science and Engineering*, vol. 101, p. 012053, 2015.

[12] O. Chubar, P. Elleaume, and J. Chavanne, "A 3D magnetostatics computer code for insertion devices," *Journal of Synchrotron Radiation*, vol. 5, pp. 481–484, 1998.

[13] E. Gmelin, M. Asen-Palmer, M. Reuther, and R. Villar, "Thermal boundary resistance of mechanical contacts between solids at sub-ambient temperatures," *Journal of Physics D: Applied Physics*, vol. 32, no. 6, p. R19, 1999.

[14] I.R. Dixon, R.P. Walsh, W.D. Markiewicz, and C.A. Swenson, "Mechanical properties of epoxy impregnated superconducting solenoids," *IEEE Transactions on Magnetics*, vol. 32, no. 4, pp. 2917–2920, 1996.